Simulation of Mass Transfer in a Microfluidic Experiment Using the Moving Mesh Method

K. R. Weisbrod*, R. M. Roberts, R. M. Chamberlin, S. L. Yarbro
Los Alamos National Laboratory
*Corresponding author: M.S. 580, Los Alamos, NM 87545, weisbrod@lanl.gov

Abstract: Multiphase flow in a microreactor was studied numerically for two immiscible liquids. Validation of the model was sought by simulating the flow behavior and mass transfer characteristics of a neutralization titration reaction described in the literature. Contact angles between the flowing phases and the wall, as well as interfacial tension and the pressure field, defined the interfacial boundary configuration. After first performing simulations to capture the velocity profile, mass transfer and reaction rates were modeled. Mass transfer between phases was determined through a measured partition coefficient. While the influence of contact angle upon extent of reaction was explored for a 2-D model, 3-D simulations more closely represented the measured reaction completion. COMSOL Multiphysics was found to effectively simulate the experiment and provides a tool for evaluating process sensitivities.

Keywords: microfluidic, mass transfer, slug flow, liquid-liquid, contact angle

1. Introduction

Two phase liquid-liquid systems are used extensively in chemical processes involving reaction engineering and separations. More recently, microreactors are being developed to exploit the very high mass transfer rates that accompany flow on the sub-millimeter scale. Liquid-liquid contact may be accomplished using parallel flow where each phase is held in place by capillary forces [1]. Segregated slug flow may provide improved mass transfer between phases through improved intra-phase mixing and shear at the interphase boundary.

Design and operation of a microreactor is complicated by numerous potential operating variables. These include flow velocity, channel size, channel geometry, slug length and liquid properties. Evaluation and correlation of the complex relationship requires an extensive set of experiments. This task can be simplified through development and validation of a numerical model that captures the fundamental physics [2].

Progress toward predicting mass transfer begins with the characterization of two-phase flow that is a function of flow velocity, channel dimensions, cross section and fluid properties. Kashid et al. [3] identified and correlated four flow regimes that were observed experimentally. At low flow rates, slug flow predominated. Annular flow occurred at the highest flow rates. Numerical modeling with ANSYS Fluent captured many of the flow characteristics. To develop correlations, mixing within each phase was modeled by Tanthapanichakoon et al. [4,5] and Rhee and Burns [6]. Kashid et al. [2] reviewed the available literature on gas-liquid and liquid-liquid mass transfer in microreactors and proposed several empirical correlations.

A definitive series of experiments were performed by Burns and Ramshaw [7] that involve extraction of acetic acid from a kerosene phase into an aqueous phase where it is neutralized. While wettability appeared to vary, a relatively complete set of data was reported that may serve to validate models. Harries et al. [8] modeled their experiments using an early version of CFX and an auxiliary Fortran program to capture mass transfer. Equal sized slugs of aqueous and organic phase, assumed to be of equal viscosity, was modeled in 2-D. Flow was simulated with a moving wall boundary condition. The interface between the two phases was linear and perpendicular to the walls. A partitioning coefficient of 85:1 in favor of the aqueous phase was assumed; apparently to match the transfer rates. The model did a surprisingly good job of matching measured titration rates.

More recently, Han and Dennis [9] created a similar model with COMSOL. A flat fluid interface and moving wall boundary condition provided predictions that were not compared to the Burns and Ramshaw experiments because of differences in flow cross section.

This paper describes work to model the Burns-Ramshaw experiments by applying the

full functionality of COMSOL to capture hydrodynamics, mass transfer rates and the neutralization reaction using all known input properties of the system. This includes solution properties, diffusion coefficients and estimated interfacial tension. Since images from their experiments appeared to exhibit multiple wettabilities, the effect of contact angle is explored.

The Burns-Ramshaw experiment consisted of a T-junction cut in glass with square channels 380 μm deep. Equal flow of kerosene and water yielded slugs of approximately equal length (Fig. 4 in Ref. 7). The kerosene phase contained 0.5 M acetic acid while the initial aqueous phase consisted of a 0.25 M solution of potassium hydroxide (KOH). Acetic acid (AA) diffused from the kerosene phase into the aqueous phase and was neutralized by KOH.

$$CH_3COOH = NaOH \rightarrow CH_3COONa + H_2O \quad (1)$$
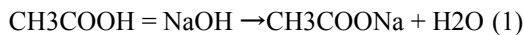
Acetic acid strongly partitioned away from the kerosene phase into water. Potassium hydroxide is essentially insoluble in kerosene.

2. Use of COMSOL Multiphysics

2.1 Model Description

An initial study of mass transport inside a square channel may be represented by a two dimensional slice. Both phases are assumed to be incompressible and Newtonian. Fluid flow is numerically represented by the Navier-Stokes equation using finite element methods with appropriate boundary conditions.

The phase field method was initially used to model slug formation and movement down the mixing channel. As described in the results section, a number of limitations of the method prevented computation of mass transfer. Subsequently, the Arbitrary Lagrangian-Eulerian (ALE) Moving Mesh method was applied to the problem. The ability to define discrete phase domains allows specification of location for a given species. It also simplifies definition of partitioning coefficients. A disadvantage of the method is that it cannot model slug formation. Consequently, the fluid velocity field and mass transfer were modeled after slug formation.

A computational domain is shown in Figure 1 where a plane of symmetry reduces element count by half. At the point where the phase boundary and wall meet, the two phase interface moves at an average velocity of the slug while maintaining a constant contact angle. Both conditions are met through use of the Navier slip boundary condition.

Figure 1. Schematic illustration of the computational configuration in 2-D.

Computation of a mass transfer rate consists of a two-step process. First the fluid flow velocity profile is calculated by modeling the flow of three slugs as they move down a channel (Figure 2).
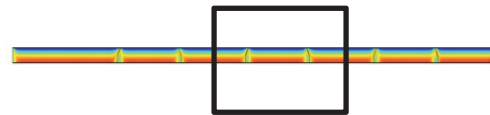

Figure 2. Selection of Step 2 input from Step 1 output with color indicating flow velocity, red - high velocity along symmetry plan and blue - low velocity at wall.

When a steady-state flow velocity is obtained in the middle slug, the simulation is stopped and the velocity profile is transferred to the second step that is treated as Component 2 in COMSOL. Flow in the x-axis direction is normalized to the slug frame of reference by subtracting the average flow velocity. Mass transfer parameters are input into this stage. Simulated flow velocities for the middle slug are plotted in Figure 3. The aqueous phase is shown with the organic phase split and joined numerically at each end by the periodic boundary condition. This condition assumes that the organic phase has undergone an insignificant change in average concentration during the time a slug moves through the length of a unit cell.
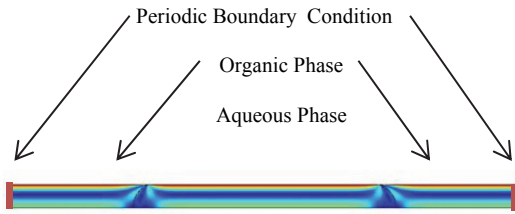
Figure 3. Layout of Step 2 phases and boundary conditions.

Under a special case, a thin film of continuous phase separates a slug from the channel wall. This condition, corresponding to a contact angle of π, may be simulated with a moving wall. A periodic boundary condition is still implemented though a two-step process is not needed.

Transport across the interface and reaction is simplified by the Moving Mesh method. The mass flux on each side of the interface is defined as

Organic phase:

$$N_{o,CAA\_o} = M^*\left(C_{AA\_o} - K^*C_{AA\_w}\right) mol/(m\ s)$$

Aqueous phase:

$$N_{o,CAA\_w} = -M^*\left(C_{AA\_o} - K^*C_{AA\_w}\right) mol/(m\ s)$$

The rate of reaction between AA and KOH is represented by a second order reaction:

$$R_{CAA,w} = R_{C\_KOH} = -k\ C_{AA\_o}\ C_{AA\_w}\ mol/(m^3 s)$$

where k = 0.1 mol/(m³·s).

2.2 Input Parameters

Parameters used in the model are given in Appendix 1. A lower interfacial tension is assumed compared to a typical kerosene / water interface as a result of the formation of natural surfactants through a saponification reaction with KOH. The partition coefficient is based on 3 to 4 percent acetic acid in kerosene in equilibrium with water. Diffusion coefficients were calculated from the Wilke-Chang correlation [10] after the Han and Dennis [9].

2.3 Meshing and Time Requirements

The simulations were performed on a 2.7 Ghz dual-processor quad-core Xeon workstation with 24GB of RAM. The Pardiso direct solver used 3 to 5 GB of RAM for 2-D simulations and 20 GB for a 3-D model as defined in Table 1. CPU usage varied from 65 to 100 percent. 3-D simulations required 20 GB of RAM. Triangular and tetrahedral meshes were applied for 2-D and 3-D cases, respectively. For 3-D simulations, memory requirements increased significantly when the cross channel dimension contained more than 10 elements. Mesh size was reduced by a factor of two at the phase boundary for all cases.

Table 1. Simulation conditions.

Mesh across channel	Number elements	Solution time (min)	Sim. end time, s	t*, Soln t/ Sim t (min/s)
Step 1- 14	30K	3.8	1	3.8
Step 2- 14	25K	6.6	10	0.7
Step 1 3-D 10x10	750K	102	0.5	60- 2000
Step 2 3-D 12x12	407K	-	-	10-140
2-D Phase- Field 24	35K to 85K	2680	3	894

A primary advantage of the two-step process with the Moving Mesh method is a reduced run time to obtain a steady state flow velocity. Once this step is completed, the number of elements may be reduced and a finer mesh may be used for the mass transport step. For 3-D simulations, that covered a wide range of average flow velocities, t* varies significantly since the time step size is limited to allow only one pore volume throughput per time step.

The phase-field method required significantly more solution time. This difference may be attributed to velocity solutions for the whole simulation time and use of the Adaptive Refinement method at the phase boundary.

3. Results and Discussion

The conservation of mass for each phase is a primary concern in modeling mass transfer in multiphase systems. For a microfluidic application, Amiri et al. [11,12] found that the phase field method, implementing Cahn-Hilliard theory, provided improved performance versus the Level Set method. Besides specifying the interfacial tension and contact angle, two other variables are introduced; the mobility parameter, γ, and capillary width, ε. While ε is generally chosen as half the maximum element size, fewer guidelines are available for γ. Figure 4 illustrates how the choice of mobility parameter can greatly impact flow behavior. Slug flow develops only when γ is in the order of 100.

(a) Mobility Parameter = 10

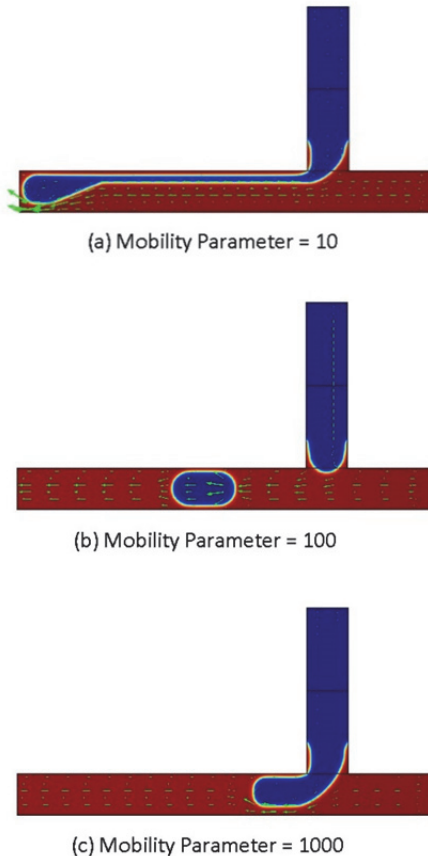(b) Mobility Parameter = 100

(c) Mobility Parameter = 1000

Figure 4. Response of phase behavior to mobility parameter variations.

A significant limitation with the phase field method was the apparent dissolution of a slug with time as it moves down the flow channel. The magnitude of the effect may be demonstrated in a result where less slug shrinkage occurred. In four seconds, the time for 80 percent reaction completion, the slug shrunk by 10 percent. Initially, this behavior was attributed to a "leaky" interface between the phases. A finer mesh or lower interfacial tension reduced the effect but not sufficiently. Yue et al. [13] described this behavior as an inherent property of the Cahn-Hilliard formulation. It was observed that while the phase interface was preserved, a finite amount of the slug phase appeared in the dispersed phase. The effect may be reduced by equal phase ratios, a finer mesh in combination with adaptive meshing, modeling slugs larger than a critical size, and choice of the mobility parameter. In this study, a set of parameters that adequately described slug behavior for longer periods and met slug shrinkage constraints could not be found. While the phase field method may prove helpful for modeling slug formation, another method is needed for mass transfer modeling.

In previous studies [8, 9], a flat interface perpendicular to the channel walls was assumed (contact angle equals $\pi/2$). A single set of circulation patterns developed in each phase with symmetry on the main axis. When a contact angle of $7\pi/8$ is introduced, the bulbous leading and trailing phase interfaces develop their own flow cell (Figure 5).
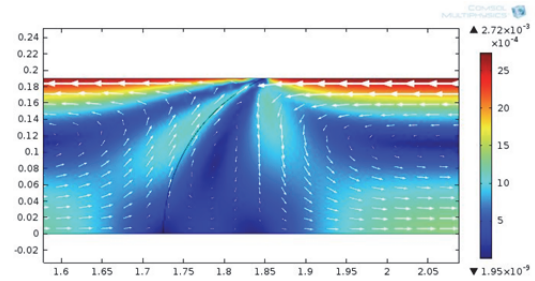

Figure 5. Flow in bulbous region; color indicates flow velocity magitude.

Drag flow along the wall creates the primary circulation. Secondary circulation develops in the bulbous zone and Figure 6 illustrates the resulting concentration distribution of AA. Preferential partitioning of AA from the organic to aqueous phase yields a higher concentration of AA in the water phase. Circulation within the bulbous zone leads to a higher local AA

concentration and slower transfer to the bulk KOH solution where it is neutralized. Conversely, the KOH is rapidly consumed in the bulbous region.
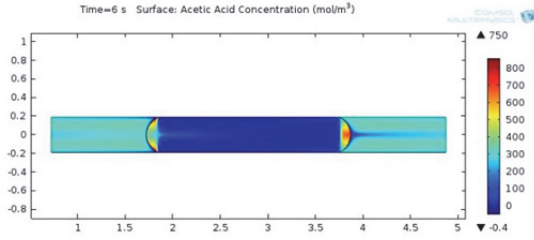

Figure 6. Acetic acid concentration distribution from 2-D model with increased concentration in bulbous region; velocity = 2.8 mm/s, t = 6 seconds.

A series of simulations were performed where the contact angle was varied from π/2 to π. Figure 7(a) illustrates the fraction KOH reacted versus time.
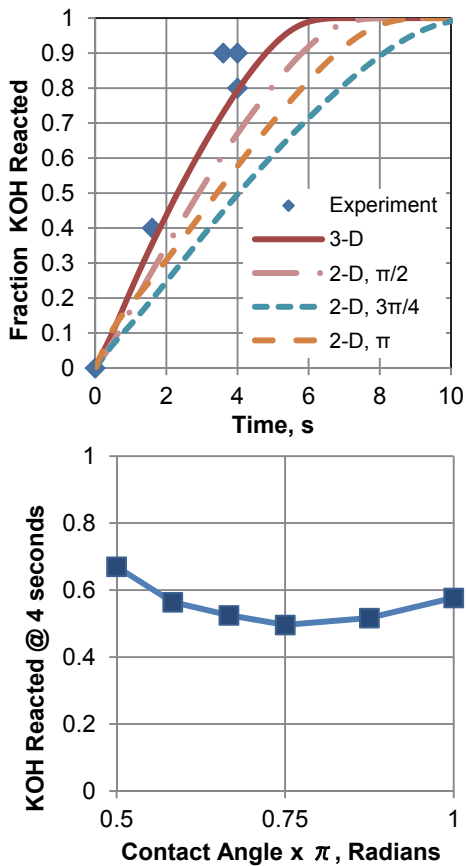

. **Figure 7.** Influence of contact angle on extent of reaction; velocity = 2.8 mm/sec.

At four seconds, reaction is highest at π/2. A minimum is observed at 3π/4. The improved fraction reacted at contact angles greater than 3π/4 may be attributed to better circulation in the bulbous zone.

The model for a contact angle of π applied a moving wall instead of Navier-slip boundary condition. The slug domain, initially introduced as an elliptical shape, rapidly displaced the organic phase near the wall, but left a thin organic film. The estimated film thickness was 2 μm. This value may be compared to the analytically derived value of 3.5 μm.[14] Under short contact times and high flow velocities, high mass transfer rates in the film region can contribute significantly to the total interphase mass transfer. In this case however, the film is too thin have a significant effect.
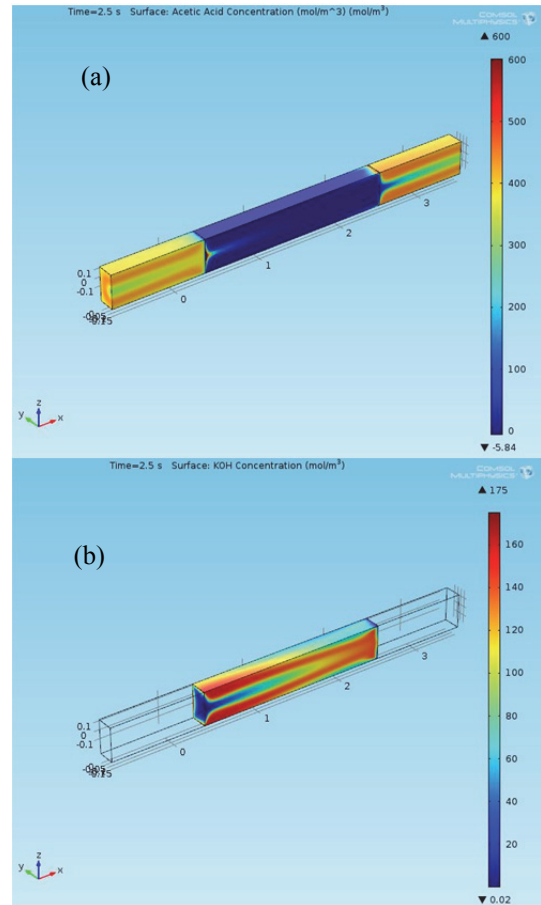

Figure 8. 3-D concentration results: (a) Acetic acid, (b) KOH , flow velocity = 2.8 mm/sec, time = 2.5 s.

Greater reaction rates are obtained with the 3-D model versus a 2-D model (Figure 7(a)). The better match with experimental results may be attributed to capturing the circulation patterns arising from the channel sides. Higher contact area per unit volume is obtained to enhance mass transport. This additional flow is apparent in the concentration profiles shown in Figure 8.

4. Conclusions

The moving mesh method can be effectively applied to model hydrodynamics and mass transfer behavior in complex systems. System variables may be explored, such as contact angle, to predict changes in conversion rates. While model sensitivities may be explored in 2-D, a full 3-D model is needed to capture conversion rates that were observed in the experiment.

5. References

1. A. Aota, K. Mawatari, T. Kitamori, Parallel multiphase microflows: fundamental physics, stabilitzation methods and applications, *Lab on a Chip*, **9**, 2470 (2009)

2. M. N. Kashid, A. Renken, L. Kiwi-Minsker, Gas-Liquid and Liquid-Liquid Mass Transfer in Microstructured Reactors, *Chem. Engr. Science*, **66**, 3876-3897 (2011).

3. Kashid, M.N., W. Kowalinski, A. Renken, J. Baldyga and L. Kiwi-Minsker, Analytical method to predict two-phase flow pattern in horizontal micro-capillaries, *Chem Eng. Sci.,* **74**, 219 (2012)

4. W. Tanthapanichakoon, N. Aoki, K Matsuyama, K. Mae, Design of mixing in microfluidic liquid slugs based on a new dimensionless number of precise reaction and mixing operations, *Chem. Eng. Sci.,* **61**, 4220 (2006)

5. W. Tanthapanichakoon, K Matsuyama, N. Aoki, K. Mae, Design of microfluidic slug mixing based on the correlation between a dimensionless mixing rate and a modified Peclet number, *Chem. Eng. Sci.,* **61**, 7385 (2006)

6. Rhee, M. and M.A. Burns, Drop Mixing in a Microchannel for Lab-on-a-chip Platforms, *Langmuir*, **24**, 590 (2008)

7. J.R. Burns and C. Ramshaw, The intensification of rapid reaction in multiphase systems using slug flow in capillaries, *Lab on a Chip*, **1**, 10 (2001).

8. N. Harries, J.R. Burns, D.A. Barrow and C. Ramshaw, A numerical model for segmented flow in a microreactor*, Int J. Heat Mass Trans.*, **46** 3313 (2003).

9. W. Han and B.H. Dennis, Numerical Investigation of Mass Transfer with Two-Phase Slug Flow in a Capillary, Proceeding of the COMSOL Conference, Boston (2010).

10. RS. Brodkey, H.C. Hershey, *Transport Phenomena: A Unified Approach,* Vol. **2**, Brodkey Publishing (1988).

11. H.A. Akhlaghi Amiri and A.A. Hamouda, Evaluation of level set and phase field methods in modeling two phase with viscosity contrast through dual-permeability porous medium, *Int. J. Multiphase Flow*, **52,** 22 (2013).

12. P.T. Yue, C. Zhou, J.J. Feng, C.F. Ollivier-Gooch and H.H. Hu, "Phase-field simulations of interfacial dynamics in viscoelastic fluids using finite elements with adaptive meshing", *J. Comp. Physics*, **219,** 47 (2006).

13. P. Yue, C. Zhou et. al., Spontaneous Shrinkage of Drops and Mass Conservation in Phase-Field Simulations, *J. Comp. Physics*, **223,** 1-9 (2007)

14. A. Ghanini, M.N. Kashid and D.W. Agar, Effective interfacial area for mass transfer in the liquid-liquid slug flow capillary microreactors, *Chem Eng. Proc.*, **49**, 358 (2010)

9. Acknowledgements

10. Appendix

Table 2: Input Parameters

Parameter	Symbol	Value
Interfacial Tension	σ	0.008 N/m
Navier slip length		0.2 h
Partition Coefficient, oil/water	K*	0.036
Stiff-spring velocity	M*	1E4 m/s
Organic phase		
Initial concentration, AA	$C_{o,AA}$	500 mol/m^3
Density	ρ	790 Kg/m^3
Dynamic Viscosity	μ	2.1 Pa·s
AA diffusivity in organic phase	D_{AA_o}	1.2E-9 m^2/s
Aqueous phase		
Initial concentration, AA	$C_{o,AA}$	0 mol/m^3
Initial concentration, KOH	$C_{o,KOH}$	250 mol/m^3
Density	ρ	998 Kg/m^3
Dynamic Viscosity	μ	1.2 Pa·s
AA diffusivity in aqueous phase	D_{AA_w}	1.3E-9 m^2/s
KOH diffusivity in aqueous phase	D_{KOH_w}	2.9E-9 m^2/s